

# Molecular Dynamics Simulation of Complex Formation by Lysine Dendrigrraft of Second Generation and Semax Peptide

I. Neelov, E. Popova

**Abstract**—Lysine dendrigrrafts are new type of branched lysine peptides similar to lysine dendrimers but having central core consisting of eight lysine aminoacid residues. Therapeutic Semax peptide are regulatory peptides consisting of seven aminoacid residues and having antioxidant, antihypoxic and neuroprotective properties. It is known that lysine dendrimers could penetrate blood brain barrier, thus it can be assumed that lysine dendrigrraft could penetrate it also and thus can be used in future for delivery of different drugs to brain. In present paper we investigated six different systems: first three systems contain 8, 16 and 24 Semax peptides and three other systems contain one lysine dendrigrraft and 8, 16 and 24 Semax peptides correspondingly. All six systems were studied in water solvent with Cl counterions using molecular dynamics simulation method. For last three systems both complexes formation and equilibrium properties of complexes were investigated. It was shown that stable complexes consisting of dendrigrraft and Semax peptides were formed in all three cases (with 8, 16 and 32 peptide molecules) and structures of these complexes were investigated. It was obtained that radius of gyration  $R_g$  of complex increase with number of peptides but shape anisotropy does not change much with size of complex.

**Keywords**—molecular dynamics simulation, lysine dendrigrraft, Semax peptides, complex formation

## I. INTRODUCTION

INTEREST to macromolecules with regular branched structure grows every year [1]. One of the most well-known polymers with dendritic structures are dendrimers. The use of different types of dendrimers in drug delivery research is discussed in many papers [2], [3]. Dendrigrraft is also a branched polymer. Dendrigrrafts could be described from one hand as dendrimers with short linear chain in their core or from another hand as dendritic brush with short main chain and long side chains. Lysine dendrigrrafts consists entirely of lysine aminoacid residues (that are biocompatible) [4], [5]. At the same time their terminal groups could be functionalized by other aminoacids or by other active groups or molecules [6]. Lysine dendrigrrafts are polymers that are rich with amines.

This work was partly supported by grant 074-U01 of Government of RF and RFBR grants 16-03-00775 and 15-33-20693mol\_a\_ved.

I.M. Neelov is with Institute of Macromolecular Compounds, Russian Academy of Sciences and ITMO, St. Petersburg, Russia (e-mail: i.neelov@mail.ru).

E. V. Popova is with ITMO University and Research Institute of Hygiene, Occupational Pathology and Human Ecology, St. Petersburg, Russia (e-mail: arabka2008@mail.ru).

Due to this reason they could be used as antibacterial [7] or antiviral agents [8]. Also they could make complexes with oppositely charged peptides due to strong electrostatic interaction between their positively charged groups ( $\text{NH}_3^+$ ) and negatively charged amino acid side groups ( $\text{COO}^-$ ) of peptides. Hydrogen bonds between dendrigrraft and peptide and hydrophobic interactions between their nonpolar groups are also important for creation of such complexes. Due to these ability to make complexes the dendrigrrafts like other dendritic molecules could be used as multifunctional nanocarriers for delivery of drug or/and other molecules [9] for treatment of various disease.

Therapeutic Semax peptide (Met-Glu-His-Phe-Pro-Gly-Pro) [10] was selected for our study as a model peptide. This peptide belongs to a class of regulatory peptides and has an antioxidant, antihypoxic and neuroprotective properties. Semax is widely used for acute ischemic stroke prevention, during traumatic brain injury treatment, recovery of a patients after a stroke, in the case of optic nerve disease and glaucoma optic neuropathy. The injected form of this drug has a low bioavailability.

The goal of this paper is to demonstrate the possibility of interaction between lysine dendrigrraft of second generation and therapeutic peptide Semax using molecular dynamics method.

## II. METHODS AND MATERIALS

### A. Molecular Dynamics Methods

Molecular dynamics (MD) method is currently the main method for simulation of polymer and biopolymer systems. The method consists in numerical solution of the classical Newton equations of motion for all atoms of the all molecules in the system. It was used first in the mid-fifties of the last century [12] for two-dimensional modeling of hard disks system (2D-model of a monoatomic gas), and then was used to simulate a variety of liquids, including water [13], [14]. In 1972 this method was first applied to the simulation of a simple model of a linear polymer chain consisting of atoms connected by rigid bonds [15]. In 1975 the dynamics of short n-alkanes was studied [16]. In subsequent years MD was used for detailed study of many specific molecules using both coarse-grained and detailed full-atomic models. The potential energy of these models usually include valence bonds, valence angles and dihedral angle energies as well as van der Waals

and electrostatic energies. The definition of parameters set adequately describing the test molecule properties (force-field) is challenging and requires the experimental data for these molecules, quantum chemical calculations as well as iterative procedures and a very large amount of machine time. These calculations can be made only by large groups of specialists. Due to this reason several packages of standard computer programs, in which these parameters are defined for quite a large range of molecules become widely used in recent years. Currently the most popular molecular modeling packages are GROMACS, AMBER, CHARMM, and some others. Our simulation was performed by molecular dynamics method using the GROMACS 4.5.6 software package [17] and one of the most modern AMBER\_99SB-ildn force fields [18].

### B. Model and Calculation Method

Modeling was performed using the molecular dynamics method for systems consisting of one lysine dendrigraft of second generation with positively charged NH<sub>3</sub><sup>+</sup> end groups, 8, 16 and 24 Semax peptides (with charge -1 each), water molecules and chlorine counterions in a cubic cell with periodic boundary conditions. The initial conformation for peptide with internal rotation angles of  $\varphi = -135^\circ$ ,  $\psi = 135^\circ$ ,  $\theta = 180^\circ$  was modeled by Avogadro chemical editor. The structures were optimized in vacuum using molecular mechanics of AMBER force field. Further energy minimizations and simulations were performed using the GROMACS 4.5.6 software package and AMBER\_99SB-ildn force fields. The potential energy of this force field consists of valence bonds and angles deformation energy, internal rotation angles, van der Waals and electrostatic interactions. The procedure of molecular dynamics simulation used for lysine dendrigraft and peptides has been described earlier (for dendrimers and linear polyelectrolytes) in [19]-[31]. In all calculations the normal conditions (temperature 300 K, pressure 1 ATM) were used. Computing resources on supercomputers "Lomonosov" were provided by supercomputer center of Moscow State University [32].

## III. RESULTS AND DISCUSSION

Snapshots of systems consisting of peptides without dendrigraft and dendrigraft of second generation and 8 peptides, ions and water during simulation are shown on Fig. 1 (water molecules are not shown clarity). It is clearly seen that at the beginning of process peptide molecules are far from dendrigraft (Fig. 1, d) and from each other (Fig. 1, a). After 30 ns (Fig. 1, e) most of peptide molecules are already adsorbed on the surface of dendrigraft. But in case of a system consisting of only peptides, we can see that molecules of Semax are still far from each other (Fig. 1, b). And in the end (Fig. 1, f) all peptide molecules in the system with dendrigraft are on its surface. We obtained the same results for systems with 16 and 24 peptides. Atoms of dendrigraft molecule are shown as beads with diameter equal to their van der Waals radii. Valence bonds of various peptides are shown with lines of different colors (backbone of each peptide is shown by thick line of the same color as valence bonds). To characterize the size of the systems during the equilibration the square of

instant gyration radius  $R_g^2(t)$  was used. It was calculated using (1):

$$R_g^2(t) = \frac{1}{M} \times \left[ \sum_{i=1}^N m_i \times |r_i(t) - R|^2 \right] \quad (1)$$

where  $R$  – is the center mass of dendrigraft,  $r_i$  и  $m_i$  – coordinates and masses of  $i$  atom correspondingly,  $N$  – is the total number of atoms in dendrigraft,  $M$  is the total mass of dendrigraft. This function was calculated using *g\_gyrate* function of GROMACS software.

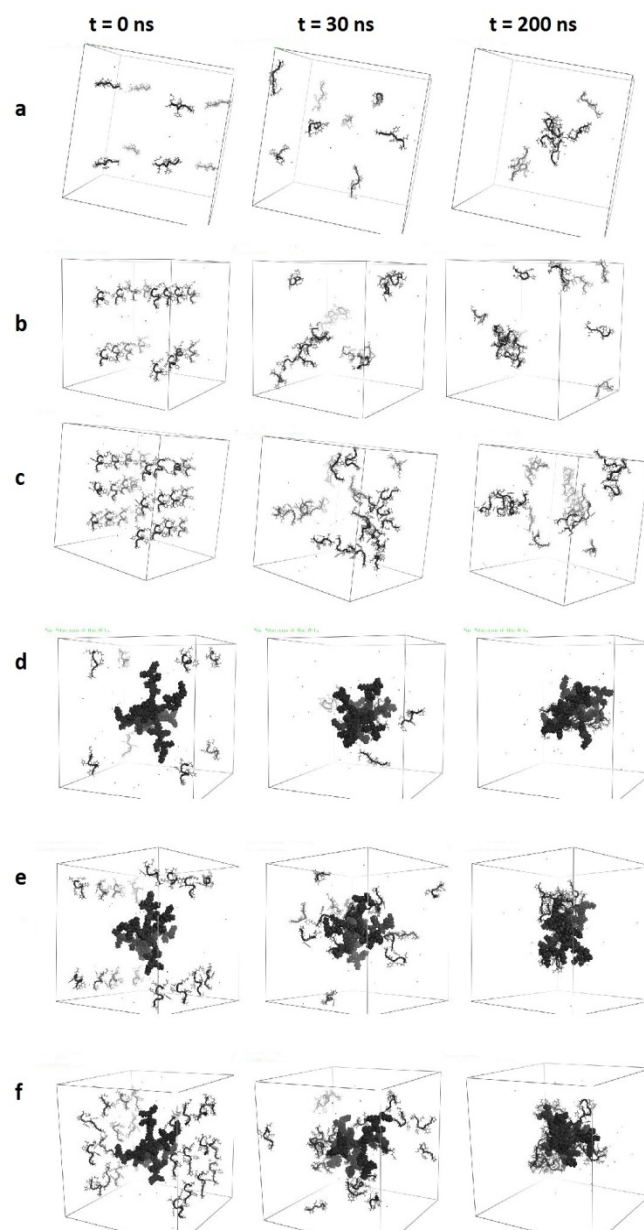


Fig. 1. Systems consisting of (from top to bottom): 8, 16 and 24 Semax peptides without dendrigraft (a-c) and dendrigraft with 8,16, and 24 Semax peptides complex formation (d-f) at three different time moments  $t=0$ ;  $t = 30$  ns;  $t = 200$  ns during complex formation

### A. Modeling of Equilibrium Process Establishment

The time dependence of gyration radius  $R_g$  at the beginning of calculation describes the process of equilibrium establishment during complex formation. It was seen that dendrigraft complex with 8 peptides forms within 20 ns. In case of 16 and 24 peptides complex with dendrigraft forms within 25 ns. After that the complexes sizes  $R_g$  fluctuate slightly, but their average value practically does not change with time. Therefore, we can assume that the systems are in equilibrium state.

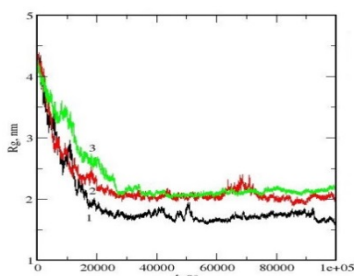


Fig. 2. System of dendrigraft DG2 and 8 Semax peptides (1), dendrigraft DG2 and 16 Semax peptides (2) and dendrigraft DG2 and 24 Semax peptides (3)

The time dependence function of distances between dendrimer and peptides (Fig. 3) demonstrates the formation of complexes. Plateau on curves of Fig. 3 means that all peptides have interacted with dendrimer molecule. This function was calculated using *g\_bond* function of GROMACS software.

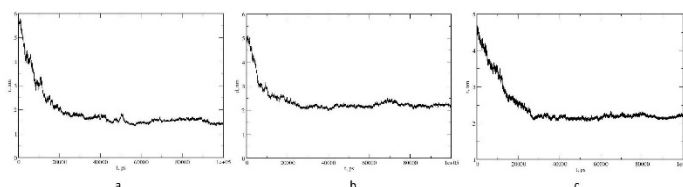


Fig. 3. Distance changes between dendrigraft and peptides: system of dendrimer DG2 and 8 Semax peptides (a); 16 Semax peptides (b); 24 Semax peptides (c)

Another quantity that can characterize the rate of complexes formation is the total number of hydrogen bonds ( $N$ ) between dendrigraft and peptides. The dependence of this value on time is shown on Fig. 4 and demonstrates how the number of specific contacts between them increases during complex formation. This function was calculated using *g\_hbonds* package of GROMACS.

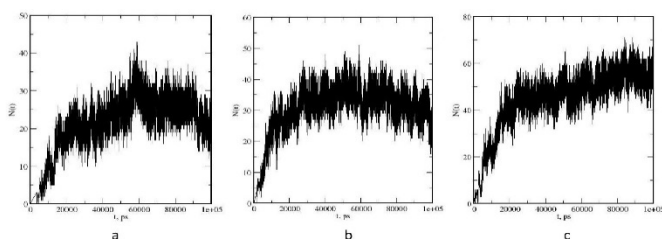


Fig. 4. Time dependence of hydrogen bonds number ( $N$ ) during the complex formation: DG2 and 8 Semax (a), DG2 and 16 Semax (b); DG2 and 24 Semax (c)

From Fig. 4 it can be concluded that the system with 8 Semax reaches equilibrium (plateau) for the first time after 20 ns. The systems with 16 and 24 peptides reach equilibrium after 25 ns. It correlates with the results of the inertia radii balance obtained during our study.

### B. Modeling of the equilibrium state

The size of complex in equilibrium state is evaluated by mean square of inertia radius averaged through the time after equilibration (2):

$$\langle R_g^2 \rangle = \frac{1}{\Delta t} \sum_{\Delta t} R_g^2(t) \quad (2)$$

where  $\Delta t = t_{\max} - t_{eq}$  and  $\langle \rangle$  means time averaging the instantaneous square of radius of gyration  $R_g^2(t)$  during equilibrium part of MD trajectory.

In equilibrium state the sizes of the first complex (DG2 and 8 Semax peptides), second complex (DG2 and 16 Semax) and third complex (DG2 and 24 Semax) are larger than the size of dendrigraft (see Table 1). It is quite natural, since it correlates with the molecular weight of the complexes increase compared to the molecular weight of the individual dendrigraft.

The shape of complex can be characterized by its tensor of inertia main component ratio ( $R_g^{11}$ ,  $R_g^{22}$ ,  $R_g^{33}$ ), that are in Table 1. For example, in the simplest case, anisotropy can be characterized by  $R_g^{33}/R_g^{11}$ . The shape of complex could be roughly characterised by ratio of largest and smallest eigenvalues of inertia tensor describing our system  $R_g^{33}/R_g^{11}$ . Calculated values of these anisotropy for our systems are presented also in Table 1. The molecular weight dependences of the anisotropy for systems are monotonous. The largest component of inertia tensor  $R_g^{33}$  of complex with 16 peptides is 1.17 times larger than this component in complex with 8 peptides. The largest component of inertia tensor  $R_g^{33}$  of complex with 24 peptides is 1.04 times larger than this component in complex with 16 peptides and is 1.22 times larger than this component in complex with 8 peptides. At the same time, the smallest component  $R_g^{11}$  of the complex with 16 peptides is just in 1.07 times larger than that component in complexes with 8 peptides. The smallest component  $R_g^{11}$  of the complex with 24 peptides is just in 1.16 and 1.25 times larger than that component in complexes with 16 and 8 peptides. Hence, the difference in anisotropy of complexes is determined mostly by the difference of the largest eigenvalues of our complexes.

Table 1. Eigenvalues  $R_g^{11}$ ,  $R_g^{22}$ ,  $R_g^{33}$  of tensor of inertia and the values of anisotropy of shape  $R_g^{33}/R_g^{11}$  in dendrigraft and three peptide complexes

System	$R_g^{11}$ (nm)	$R_g^{22}$ (nm)	$R_g^{33}$ (nm)	$R_g$ (nm)	$R_g^{33}/R_g^{11}$
DG2	1.12	1.45	1.51	1.67	1.35
DG2+8Semax	1.20	1.40	1.57	1.75	1.31
DG2+16Semax	1.29	1.75	1.84	2.03	1.42
DG2+24Semax	1.50	1.77	1.91	2.14	1.27

The distribution function  $p(R_g)$  of gyration radius  $R_g$  (Fig.5) gives more detailed information about the variation of  $R_g$  of dendrigraft-peptides complex and the amplitude of its fluctuations. Absence of big "tails" of  $p(R_g)$  function at high  $R_g$  values in complex indicates that peptides seem to be associated with dendrigraft rather well.

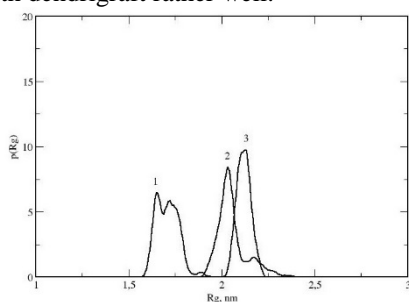


Fig. 5. Distribution function  $p(R_g)$  of gyration radius  $R_g$ : complex DG2 and 8 Semax (1); complex DG2 and 16 Semax (2); complex DG2 and 24 Semax (3)

Information about the internal structure of the equilibrium complex could be obtained using radial density distribution (3) of different groups of atoms relatively center of inertia of system. These radial distribution functions (not normalized) are shown on Fig. 6. They were calculated using  $g\_rdf$  function of GROMACS.

Fig. 6 demonstrates that dendrigraft (curve 2) is located in the center of the complexes and peptides (curve 1) mainly on the surface of complex in both systems. At the same time, some fraction of peptides could slightly penetrate into outer part of dendrigraft but not to its inner part (see Fig. 6).

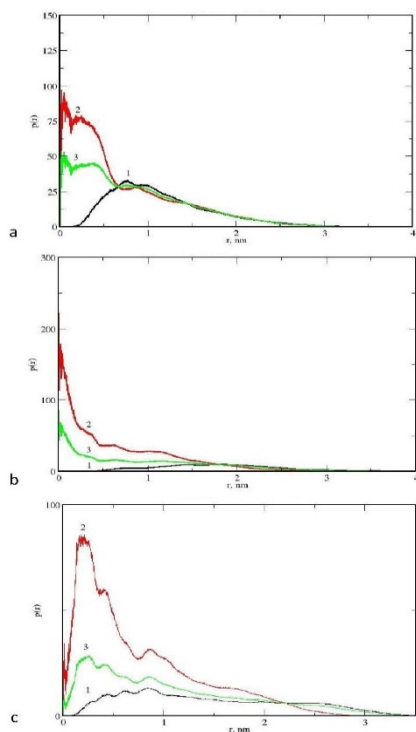


Fig. 6. Radial distribution  $p(r)$  curves: dendrigraft DG2 and 8 Semax (a), dendrigraft DG2 and 16 Semax (b), dendrigraft DG2 and 24 Semax (c). Distribution curves: peptide atoms (1); dendrimer atoms (2); all atoms of complex (3)

The number of hydrogen bonds between peptides and dendrigraft shows how tightly peptides associate with dendrigraft. From Fig. 4 it follows that average hydrogen bonds number in equilibrium state ( $t > 20$  ns) for DG2 + 8 Semax complex is equal to 25. Average hydrogen bonds number in equilibrium state ( $t > 25$  ns) for DG2 + 16 Semax and for DG2 + 24 Semax complexes was equal to 35 and 52.

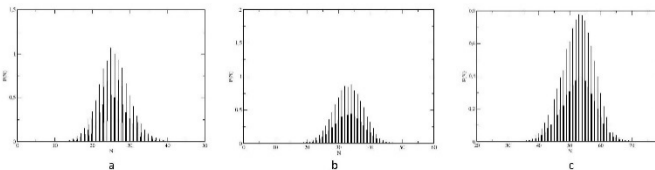


Fig. 7. The distribution function  $P(N)$  of hydrogen bonds number  $N$  of complexes: complex DG2 and 8 Semax (a); complex DG2 and 16 Semax (b); complex DG2 and 24 Semax (c).

The distribution function of hydrogen bonds number (Fig. 7) shows how the number of hydrogen bonds in the equilibrium state can fluctuate relative to the average value. We obtained that the resulting function for the first complex has a peak of numbers of bonds that is 25. The resulting function for the second complex has a peak of numbers of bonds that is 35. The resulting function for the third complex has a peak of numbers of bonds that is 52. Thus number of hydrogen bonds between dendrimer and peptides increase slower than number of peptides in systems. It means that in systems with more peptides the contacts between dendrimer and peptides not so close as in smaller systems. All functions are quite symmetrical. Fluctuations in hydrogen bonds number are for the first system in the range of 15-40, for the second system in the range of 19-48 and for the third system in the range of 35-70.

The other characteristic of interaction between dendrigraft and peptides in complex is the distribution of ion pairs number between their charged groups (Fig. 8). It can be seen that number of ion pairs between positively charged groups ( $\text{NH}_3^+$ ) of dendrigraft and negatively charged groups ( $\text{COO}^-$ ) of the glutamic acid in peptides (curve 1) in all complexes is much higher than between dendrigraft and  $\text{Cl}^-$  counterions (curve 2).

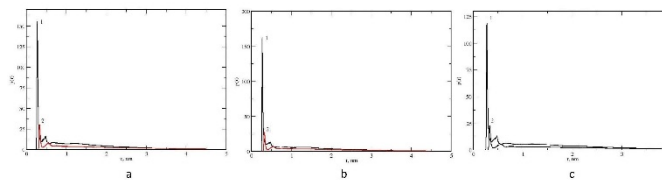


Fig. 8. Function of ion pairs radial distribution: a – DG2+8Semax, b – DG2+16Semax, c – DG2+24Semax. 1 -  $\text{NH}_3^+$  groups of dendrigraft and  $\text{COO}^-$  groups of peptides, 2 -  $\text{NH}_3^+$  groups of dendrigraft and  $\text{Cl}^-$  ions.

To evaluate the translational mobility of our systems, the time dependence of the mean square displacements (4) of the centers of inertia (MSD), were calculated. MSD was calculated using  $g\_msd$  function of GROMACS. Graphs are not shown in this paper.

$$\left\langle \sum_t \Delta r^2(t+k\Delta t) \right\rangle = \left\langle \sum_t (r(t+k\Delta t) - r(t))^2 \right\rangle = 6Dt \quad (4)$$

We have found that dependence of MSD function on time is almost linear (Fig. 9) in some interval of time  $t$  in double logarithm coordinates (not shown).

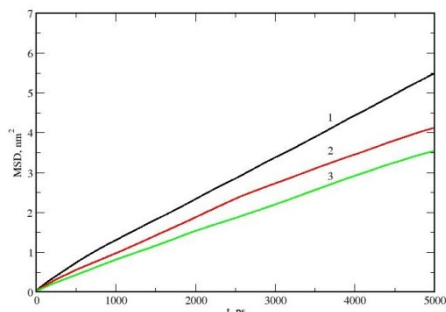


Fig. 9. Mean square displacements of the centers of inertia: complex of DG2 and 8 Semax (1), complex of DG2 and 16 Semax (2), complex of DG2 and 24 Semax (3)

It means that in this interval the motion of complex is the diffusion-like motion. Coefficient of translational diffusion of the first complex (DG2 and 8 Semax) was determined from the slope of the obtained time dependence of MSD for system and was  $D = 0.18 \pm 0.01 \text{ sm}^2/\text{s}$ . Coefficient of translational diffusion of the second complex (DG2 and 16 Semax) was determined from the slope of the obtained time dependence of MSD for system and was  $D = 0.13 \pm 0.03 \text{ sm}^2/\text{s}$ . Coefficient of translational diffusion of the third complex (DG2 and 24 Semax) was determined from the slope of the obtained time dependence of MSD for system and was  $D = 0.12 \pm 0.01 \text{ sm}^2/\text{s}$ .

### CONCLUSION

The process of complex formation by lysine dendrigraft of second generation and therapeutic Semax peptides (8, 16 and 24 molecules) and the equilibrium structures of complexes were investigated by the method of molecular dynamics simulation. Systems consisting of second generation dendrigraft with 8, 16 and 24 Semax molecules in water were studied. It was shown that the size of subsystem containing dendrigraft and peptides decrease with time rather quickly (for 20-40 ns) for all three systems containing dendrigraft and peptides. The time dependence function of distances between dendrimer and peptides and number of hydrogen bonds between dendrigraft and peptides also quickly change within this time. Taking into account all these dependences we can conclude that formation of complexes in all systems occur within 20-40 ns.

The equilibrium size (radius of gyration) of complexes increase with number of peptides in it while the shape anisotropy of complexes is fluctuate but is always close to value equal to 1.3. The density distribution function in complexes shows that dendrigraft in all three cases is mainly inside the complexes, while the peptides are more close to dendrigraft surface. The number of hydrogen bonds between dendrimer and peptides increase slower than number of

peptides in system. The number of ion pairs between positively charged  $\text{NH}_3^+$  groups of dendrigraft and  $\text{COO}^-$  carboxyl groups of glutamic acid of Semax peptides in all systems is significantly more than number of ion pairs between  $\text{NH}_3^+$  groups of the dendrigraft and chloride counterions.

### ACKNOWLEDGMENT

This work was partly supported by grant 074-U01 of Government of RF and RFBR grants 16-03-00775. Computing resources on supercomputers "Lomonosov" were provided by supercomputer center of Moscow State University [32].

### REFERENCES

- [1] J.M.J. Fréchet and D.A. Tomalia, "Dendrimers and Other Dendritic Polymers", Eds. John Wiley & Sons Ltd.:West Sussex, 2001.
- [2] R.G. Denkwalter, J. Kolc, W.J. Lukasavage, Macromolecular Highly Branched Homogeneous Compound, 1983, US Patent № 4410688.
- [3] C.C. Lee, J.M.J. Fréchet, "Synthesis and Conformations of Dendronized Poly-L-Lysine", *Macromolecules*, vol. 39, 2006, pp. 476-481.
- [4] H. Cottet, M. Martin, A. Papillaud, E. Souaid, H. Collet, A. Commeyras, "Determination of dendrigraft poly-L-lysine diffusion coefficients by Taylor dispersion analysis", *Biomacromolecules*, vol. 8, 2007, pp. 3235-3243.
- [5] H. Collet, E. Souaid, H. Cottet, A. Dératani, L. Boiteau, G. Dessalces, J.-C. Rossi, A. Commeyras, R. Pascal, "Expeditious, multigram scale synthesis of lysine dendrigraft (DGL) polymers by aqueous *N*-carboxyanhydride polycondensation", *Chem. Eur. J.*, vol. 16, 2010, pp. 2309-2316.
- [6] J.-C. Rossi, L. Boiteau, H. Collet, B.M. Tsamba, N. Larcher, R. Pascal, "Functionalisation of free amino groups of lysine dendrigraft (DGL) polymers", *Tetrahedron Letters*, vol. 53, 2012, pp. 2976-2979.
- [7] F. Oukacine, B. Romestand, D.M. Goodall, G. Massiera, L. Garrelly, H. Cottet, "Study of Antibacterial Activity by Capillary Electrophoresis Using Multiple UV Detection Points", *Anal. Chem.*, vol. 84, 2012, pp. 3302-3310.
- [8] A. Cadriere, B. Couturaud, J. Boismard, P. Le Cann, A. Gerard, A. Mas, C. Faye, L. Garrelly, B. Roig, "Assessment of poly-L-lysine dendrigrafts for virus concentration in water: use of MS2 bacteriophage as proof of concept", *Journal of Applied Microbiology*, vol. 115, 2013, pp. 290 - 297.
- [9] J. Li, Y. Guo, Y. Kuang, S. An, H. Ma, C. Jiang, "Choline transporter-targeting and co-delivery system for glioma therapy", *Biomaterials*, vol. 34, 2013, pp. 9142-9148.
- [10] M.S. Shyphshyna, N.S. Veselovsky, N.F. Myasoedov, S.I. Shram, S.A. Fedulova, "Effect of peptide Semax on synaptic activity and short-term plasticity of glutamatergic synapses of co-cultured dorsal root ganglion and dorsal horn neurons", *Fiziol Zh.*, vol. 61, 2015, pp. 48-55.
- [11] E.V. Popova, O.V. Shavykin, I.M. Neelov, F. Leermakers, (2016) "Molecular dynamics simulation of lysine dendrimer and Semax peptides interaction", *Scientific and Technical Journal of Information Technologies, Mechanics and Optics*, vol. 16, 2016, pp. 716-724.
- [12] B.J. Alder and T.E. Wainwright, "Molecular Dynamics by Electronic Computers" in *International Symposium on Transport Processes in Statistical Mechanics*, I. Prigogine, Eds. New York: John Wiley Int., 1957, pp. 97-131.
- [13] L. Verlet, "Computer "experiments" on classical fluids. I. Thermodynamical properties of Lennard-Jones molecules", *Phys. Rev.*, vol. 159, 1967, pp. 98-103.
- [14] A. Rahman, F.H. Stillinger, "Molecular dynamics study of temperature effects on water structure and kinetics", *J Chem Phys*, vol. 57, 1972, pp. 1281-1292.
- [15] M.N.K. Balabaev, A.G. Gritsov, E.E. Shnol, "Numerical modeling of motion of molecules. Motion of isolated polymer chain", *Institute of Applied Mathematics* 4, vol. 38, 1972.

- [16] J.P. Ryckaert, G. Ciccotti, H.V.C. Berendsen, "Numerical integration of Cartesian equations of motion of systems with constraints-molecular dynamics of n-alkanes", *J Comput Phys*, vol. 23, 1977, pp. 327-341.
- [17] B. Hess, C. Kutzner, D. Spoel, E. Lindahl, "GROMACS 4: Algorithms for highly efficient, load-balanced, and scalable molecular simulation", *Journal of Chemical Theory & Computation*, vol. 4, 2008, pp. 435-447.
- [18] V. Hornak, R. Abel, A. Okur, D. Strockbine, A. Roitberg, C. Simmerling, "Comparison of multiple amber force fields and development of improved protein backbone parameters", *Proteins: Structure Function and Genetics*, vol. 65, 2006, pp. 712-725.
- [19] I.M. Neelov, D.A. Markelov, S.G. Falkovich, M.Y. Ilyash, B.M. Okrugin, A.A. Darinskii, "Mathematical Simulation of Lysine Dendrimers. Temperature Dependences", *Polymer Science*, vol. 55, 2013, pp. 154-161.
- [20] S. Falkovich, D. Markelov, I. Neelov, A. Darinskii, "Are structural properties of dendrimers sensitive to the symmetry of branching? Computer simulation of lysine dendrimers", *Journal of Chemical Physics*, vol. 139, 2013, pp. 064903.
- [21] I. Neelov, S. Falkovich, D. Markelov, E. Paci, A. Darinskii, H. Tenhu, "Molecular Dynamics of Lysine Dendrimers" in *Computer Simulation and NMR. Dendrimers in Biomedical Applications*, Eds. London, 2013, pp. 99-114.
- [22] I.M. Neelov, A. Janaszewska, B. Klajnert, M. Bryszewska, N. Makova, D. Hicks, N. Pearson, G.P. Vlasov, M.Y. Ilyash, D.S. Vasilev, N.L. Dubrovskaya, L.A. Zhuravin, A.J. Turner, N.N. Nalivaeva, "Molecular properties of lysine dendrimers and their interactions with Ab-peptides and neuronal cells", *Current Medical Chemistry*, vol. 20, 2013, pp. 134-143.
- [23] I.M. Neelov, A.A. Mistonova, A.Y. Khvatov, V.V. Bezrodnij, "Molecular dynamic simulation of peptide polyelectrolytes", *Scientific and Technical Journal of Information Technologies, Mechanics and Optics*, vol. 4, 2014, pp. 169-175.
- [24] M.A. Mazo, M.Y. Shamaev, N.K. Balabaev et al Conformational mobility of carbosilane dendrimer: Molecular dynamics simulation, *Physical Chemistry and Chemical Physics*, vol. 6, 2004, pp. 1285-1289.
- [25] D.A. Markelov, S.G. Falkovich, I.M. Neelov, M.Y. Ilyash, V.V. Matveev, E. Lahderanta, P. Ingman, A.A. Darinskii, "Molecular Dynamics Simulation of Spin-lattice NMR Relaxation in Poly-L-lysine Dendrimers. Manifestation of the Semiflexibility Effect", *Physical Chemistry and Chemical Physics*, vol. 17, 2014, pp. 3214-3226.
- [26] J. Ennari, M. Elomaa, I. Neelov, F. Sundholm, "Modelling of water free and water containing solid polyelectrolytes", *Polymer*, vol. 41, 2000, pp. 985-990.
- [27] J. Ennari, I. Neelov, F. Sundholm, "Comparison of Cell Multipole and Ewald Summation Methods for Solid Polyelectrolyte", *Polymer*, vol. 41, 2000, pp. 2149-2155.
- [28] J. Ennari, I. Neelov, F. Sundholm, "Molecular Dynamics Simulation of the PEO Sulfonic Acid Anion in Water", *Comput Theor Polym Sci*, vol. 10, 2000, pp. 403-410.
- [29] J. Ennari, I. Neelov, F. Sundholm, "Molecular dynamics simulation of the structure of PEO based solid polymer electrolytes", *Polymer*, vol. 41, 2000, pp. 4057-4063.
- [30] J. Ennari, I. Neelov, F. Sundholm, "Estimation of the ion conductivity of a PEO-based polyelectrolyte system by molecular modeling", *Polymer*, vol. 42, 2001, pp. 8043-8050.
- [31] J. Ennari, I. Neelov, F. Sundholm, "Modelling of gas transport properties of polymer electrolytes containing various amount of water", *Polymer*, vol. 45, 2004, pp. 4171-4179.
- [32] V. Sadovnichy, A. Tikhonravov, V. Voevodin, V. Opanasenko, *Contemporary High Performance Computing: From Petascale toward Exascale*, Eds. Boca Raton, 2013, pp. 283-307.